Extraction of River Networks from Satellite Images by Combining Mathematical Morphology and Hydrology

Pierre Soille and Jacopo Grazzini

Spatial Data Infrastructures Unit
Institute for Environment and Sustainability
DG Joint Research Centre, European Commission, I-21020 Ispra, Italy
{Pierre.Soille,Jacopo.Grazzini}@jrc.it

Abstract. In this paper, we propose a new methodology for extracting river networks from satellite images. It combines morphological generalised geodesic transformations with hydrological overland flow simulations. The method requires the prior generation of a geodesic mask and a marker image by applying a series of transformations to the original image. These images are then combined so as to produce a pseudo digital elevation model whose valleys match the desired networks. The performance of the methodology is demonstrated for the extraction of river networks from a single band of a Landsat image. The method is generic in the sense that it can be extended for the extraction of other types of arborescent networks such as blood vessels in medical images.

1 Introduction

Line networks [1], also called thin nets [2] or curvilinear structures [3], are found in numerous applications fields. Probably the most studied ones are those encountered in medical images (e.g., blood vessels [4]) and satellite images of the Earth (e.g., roads [5,6] and rivers [7,8,9]). The extraction of line networks is often based on a two step approach. Typically, a segmentation and/or classification leads to an initial detection of the desired network avoiding false positive detections but containing gaps. These gaps are then bridged using perceptual grouping techniques.

In this paper, we focus on the extraction of river networks in satellite images and propose to exploit the arborescent nature of these networks (i.e., tree-like structure with a root). Similarly to the watershed based segmentation, this is achieved by combining concepts arising from mathematical morphology and hydrology. Morphological algorithms allow for the creation of a pseudo digital elevation model whose main valley lines match actual rivers. These valleys are then extracted using overland flow simulation procedures known in hydrology.

The rest of the paper is organised as follows. Background morphological and hydrological concepts at the root of the proposed methodology are recalled in Sec. 2. The methodology itself is detailed in Sec. 3.

W.G. Kropatsch, M. Kampel, and A. Hanbury (Eds.): CAIP 2007, LNCS 4673, pp. 636–644, 2007.

2 Background Concepts

This section briefly describes the two main concepts at the basis of the proposed methodology: geodesic time function in mathematical morphology and contributing drainage areas in hydrology. Unless otherwise stated, we adopt definitions and notations presented in [10].

2.1 Geodesic Time in Mathematical Morphology

The geodesic distance between two points of a connected set is defined as the length of the shortest path(s) linking these points and remaining in the set [11]. This idea has been generalised to grey tone geodesic masks in [12] by introducing the notion of geodesic time. The time necessary for travelling a path is defined as the sum of the intensity values of the points of the path. The geodesic time separating two points of a grey tone geodesic mask is then defined as the smallest amount of time of all paths linking these points and remaining within the definition domain of the geodesic mask.

Formally, the *time* necessary to cover a discrete path $\mathcal{P}$ of length l (i.e., $\mathcal{P} = (p_o, \ldots, p_l)$) defined on a discrete grey scale image f equals the mean of the values of f taken two at a time along $\mathcal{P}$. It is denoted by $\tau_f(\mathcal{P})$:

$$\tau_f(\mathcal{P}) = \sum_{i=1}^{l} \frac{f(p_{i-1}) + f(p_i)}{2} = \frac{f(p_0)}{2} + \frac{f(p_l)}{2} + \sum_{i=1}^{l-1} f(p_i).$$

The geodesic time separating two points p and q in a grey scale image f is denoted by $\tau_f(p,q)$: $\tau_f(p,q) = \min\{\tau_f(\mathcal{P}) \mid \mathcal{P}$ is a path linking p to $q\}$. The geodesic time between a point p and a reference set of points Y of a geodesic mask image f is the smallest amount of time allowing to link p to any point q of Y:

$$\tau_f(p, Y) = \min_{q \in Y} \tau_f(p, q).$$

If p belongs to Y, the geodesic time from p to Y is zero. The geodesic time function from a reference set Y within a geodesic mask image f is defined by associating each point of the image definition domain with its geodesic time to Y. We denote by $\mathcal{T}_f(Y)$ the resulting geodesic time function:

$$\left[\mathcal{T}_f(Y)\right](p) = \tau_f(p, Y).$$

An efficient algorithm based on priority queue data structures is detailed in [10, pp. 237–238]. Note that the concept of geodesic time function is closely related to the notion grey weighted distances in image processing [13] and, more generally, cost functions in digital graphs.

2.2 Contributing Drainage Area in Hydrology

Digital elevation models (DEMs) can be viewed as grey tone images where the intensity value of each pixel represents the elevation of the terrain at the corresponding location. Since the availability of the first DEMs in the early 80's, numerous methodologies have been proposed for extracting river networks from them. A recent survey on this topic can be found in [14]. The best available method relies on the simulation of the flow of water on the topographic surface. It assumes that (i) all spurious minima have been suppressed beforehand and (ii) every point except the stream outlets have at least one neighbour with a lower elevation than the considered point. The flow direction at each point is then defined as the direction of the 8-neighbour of the point corresponding to the steepest slope. In this sense, each point of the terrain belongs to the network of streams. This is a valid assumption since the notion of stream is dynamic and depends on the intensity of the rain over the terrain so that for heavy rainfall all points of the terrain are flowing. In practice, the flow directions allow for the computation of the number of pixels located upstream of each point of the DEM. This number is called *contributing drainage area*. River network pixels are then defined as those pixels whose contributing drainage area exceeds some threshold value, see for example [15] and references thereof.

3 Methodology

Our methodology for extracting river networks from a single optical satellite image can be summarised as follows:

1. Define the outlets of the desired river network and a region of interest;
2. Enhance potential river stretches;
3. Generate a pseudo DEM by computing the geodesic time function with the outlets as reference set and the image with enhanced rivers as geodesic mask;
4. Calculate the local flow directions of the pseudo DEM and the subsequent contributing drainage areas;
5. Trim the resulting space filling network so as to obtain a network matching the target network.

The successive steps are detailed below and illustrated on the Landsat image displayed in Fig. 1a.

3.1 Outlet Definition and Region of Interest

Typically, the outlets of the target network correspond to the sea pixels of the input imagery. Hence, the sea pixels play the role of the reference set of the geodesic time function and will therefore correspond to the level 0 of the pseudo DEM generated in Sec. 3.3. If the watershed boundaries of the catchment basins of the processed area are available, all computations are restricted to a region of interest defined as the union of the catchments fully included in the image and flowing towards sea pixels. Alternatively, other water features such as large inland lakes can be used instead of the sea for the reference set. Eventually, if no such features can be detected, the boundary of the image definition domain can be considered as a valid outlet in a first approximation.

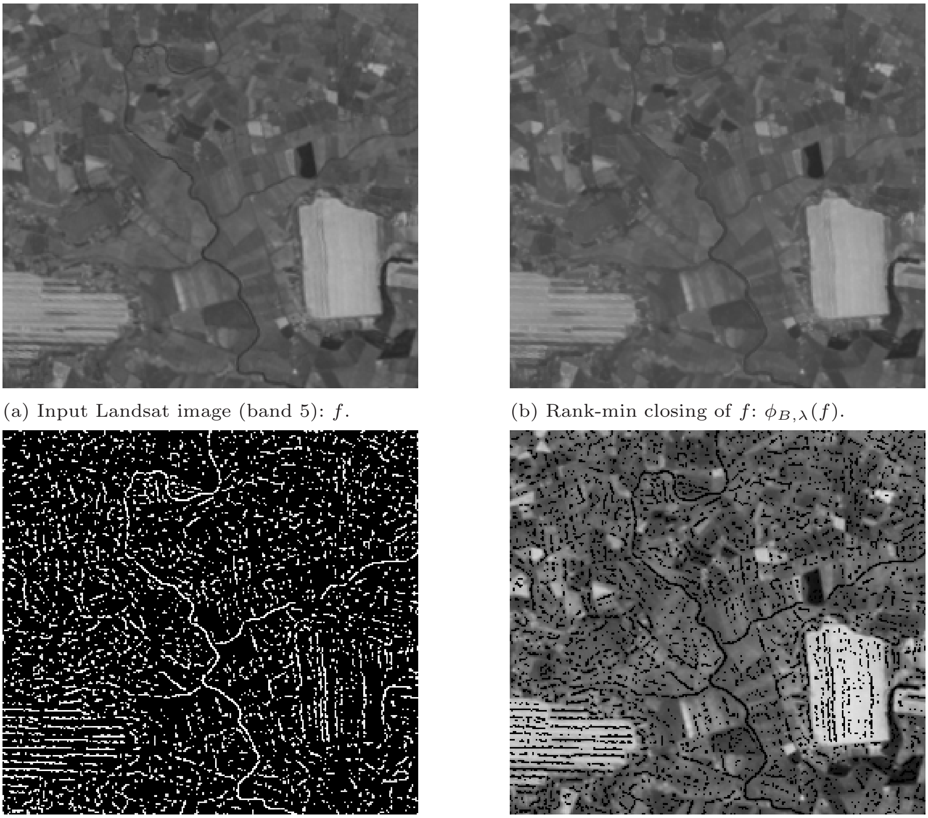

(a) Input Landsat image (band 5): f.

(b) Rank-min closing of f: $\phi_{B,\lambda}(f)$.

(c) Top-hat of f: $\mathrm{BTH}(f) = f - \phi_{B,\lambda}(f)$.

(d) Geodesic mask: $g = f \cdot T_{[0,0]}(\mathrm{BTH}(f))$.

Fig. 1. Geodesic mask creation from the fifth band of a Landsat image

3.2 Generation of Geodesic Mask

The geodesic mask is obtained by modifying the input image in such a way that potential river pixels are set to low values. By doing so, the geodesic time function will propagate faster along potential rivers. Since satellite images are usually multispectral images, a combination of channels can be used. In this paper, we use a single spectral band having low reflectance values for water (alternatively, band combinations such as those defined by a water index could be used). Then, rather than exploiting knowledge about the reflectance values of water in the selected band, we translate knowledge about the shape, size, and local contrast of river stretches into a series of morphological operations. By doing so, we are able to enhance river stretches that could not be detected solely on the basis of their spectral values. Indeed, many rivers are detectable by a human operator owing to their shape and relative contrast since they appear as dark networks of thin lines. In mathematical morphology terms, the extraction of potential river pixels can be achieved by initially suppressing these networks with a closing by

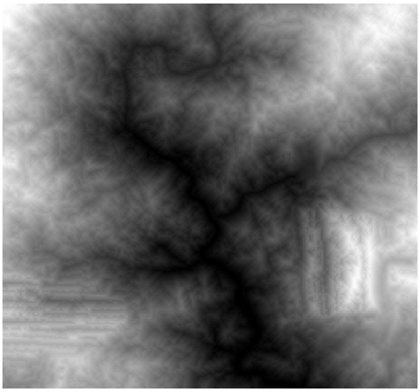

(a) Geodesic time function: $\mathcal{T}_g(\text{sea})$. This function can be seen as a pseudo DEM.

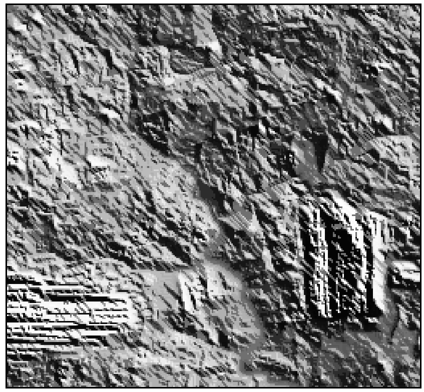

(b) Shaded view of lower complete transformation of $\mathcal{T}_g(\text{sea})$.

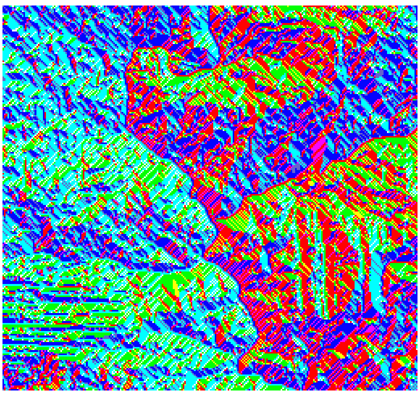

(c) Flow directions of *(b)*.

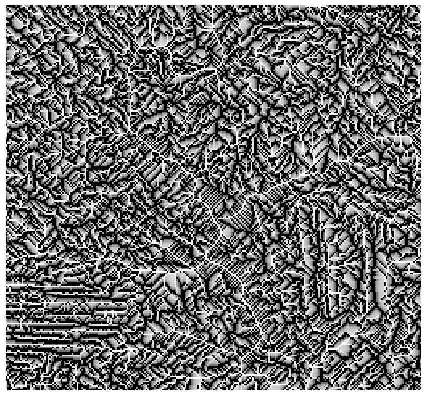

(d) Contributing drainage areas of *(c)*.

Fig. 2. From geodesic time function to contributing drainage areas (see also Fig. 1). In this example, the sea pixels are falling outside the image frame.

a disk shaped structuring element whose diameter slightly exceeds the width of the targeted network. However, a closing by a plain structuring element would enhance too many structures. A less restrictive closing consists in considering the intersection (i.e., point-wise minimum) of the closing by all subsets of the disk containing a fixed number of pixels, see Fig. 1b. This type of closing is known as a parametric closing or rank-min closing owing to its representation in terms of a rank filter followed by a point-wise minimum with the input image (see [16] and references thereof). In Fig. 1b, taking into account the physical size of a pixel, we used a 3×3 square structuring element B and considered every subset of B containing 6 pixels. Although the closed image looks very similar to the input image, this operation closes many potential river stretches. This is highlighted by computing the difference between the closing and the input image called top-hat by closing, see Fig. 1c. Notice that the top-hat by closing leads to many false positive detections. This is however not an issue because the subsequent steps cope with false positives provided that higher rate of detection are obtained for actual river stretches. We therefore consider as potential river all pixels of this top-hat by closing that have a positive response. The geodesic mask is then formed by setting to zero these pixels, all other pixels retaining their original value, see Fig. 1d.

3.3 Geodesic Time Function

The geodesic time function is then computed from the marker set (sea pixels) within the geodesic mask. Since potential river pixels are set to zero in the geodesic mask, the propagation goes faster along potential rivers so that the resulting geodesic time function mimics a digital elevation model of the studied terrain. However, the computed time values correspond to a sum of reflectance values so that they do not match actual elevations. For this reason we call this geodesic time function a *pseudo* DEM, see Fig. 2a.

(a) River network extracted by applying a fixed threshold of 23000 pixels to Fig. 2d.

(b) Extracted network overlaid on input image.

Fig. 3. River network resulting from thresholding the contributing drainage areas of the geodesic time function

3.4 From Geodesic Time Function to Drainage Areas

We then compute the flow directions on the geodesic time function. The flow direction of a pixel is defined for each pixel as the direction of the 8-neighbour producing the steepest slope. Ties are solved either by randomly selecting a possible direction or choosing the central direction when there are three adjacent possibilities. However, flow directions cannot be defined from a local neighbourhood on plateaus (resulting from the presence of zero valued pixels in the geodesic mask). Plateaus can be suppressed using geodesic distance computations from their descending border [17]. A shaded view of the resulting lower complete function is shown in Fig. 2b and the corresponding flow directions in Fig. 2c.

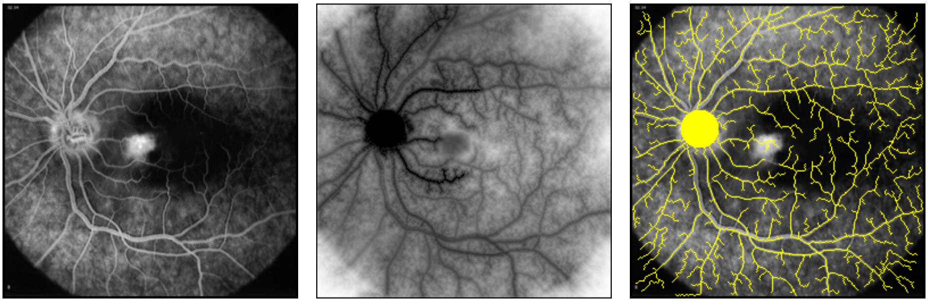

(a) Retina image. (b) Pseudo DEM. (c) Extracted network.

Fig. 4. Detection of blood vessels in an image of an eye retina using the methodology described in this paper: preliminary results

Contributing drainage areas are then calculated by simulating the flow of water on the pseudo DEM using the previously defined flow directions, see [15] for a fast algorithm. The contributing drainage areas of our sample image are displayed in Fig. 2d.

3.5 Network Extraction

The extraction of an actual network from the contributing drainage area image can be achieved by thresholding it for a fixed threshold value. This is illustrated in Fig. 3. Rather than using fixed thresholds, adaptive threshold values can be defined using a priori knowledge or further transformations of the input image. By doing so, the river network is defined as the downstream of all pixels whose contributing drainage area exceed their threshold value. This idea has already been used for the extraction of river networks from *actual* DEMs in [18].

4 Conclusion and Perspectives

The originality of the method proposed in this paper lies in the combination of geodesic time computations with concepts related to overland flow simulation. The generation of the pseudo digital elevation model exploits information on the local contrast (river stretches are darker in the selected band) and shape (linear and thin structures) of the targeted network as well as its arborescent organisation. If necessary, physical image formation models and the use of several spectral bands rather than a single one could be used to constrain further the generation of the pseudo DEM and/or the extraction of the final network from this DEM.

The proposed methodology is generic in the sense that it can be extended for the extraction of other arborescent networks such as blood vessels in medical images. An example of preliminary result for the extraction of blood vessels in retina images is displayed in Fig. 4. In this example, the optical nerve plays the role of the 'sea' pixels and has been set manually, see yellow disk in Fig. 4b.

All concepts are directly applicable to 3-dimensional images. This general framework will be detailed in a subsequent paper and will include the treatment of anastomoses (i.e., networks in which line features both branch out and reconnect such as for braided rivers). Multiscale concepts could also be considered for the enhancement of potential network stretches [19].

References

1. Geusebroek, J.M., Smeulders, A., Geerts, H.: A minimum cost approach for segmenting networks of lines. Int. J. of Computer Vision 43, 99–111 (2001)
2. Armande, N., Montesinos, P., Monga, O.: Thin nets extraction using a multi-scale approach. Computer Vision and Image Understanding 73, 285–295 (1999)
3. Steger, C.: An unbiased detector of curvilinear structures. IEEE Trans. on Pattern Analysis and Machine Intelligence 20, 113–125 (1998)
4. Zana, F., Klein, J.C.: Segmentation of vessel-like patterns using mathematical morphology and curvature evaluation. IEEE Trans. on Image Processing 10, 1010–1019 (2001)
5. Merlet, N., Zerubia, J.: New prospects in line detection by dynamic programming. IEEE Trans. on Pattern Analysis and Machine Intelligence 18, 426–431 (1996)
6. Mena, J.: State of the art on automatic road extraction for GIS update: A novel classification. Pattern Recognition Letters 24, 3037–3058 (2003)
7. Haralick, R., Wang, S., Shapiro, L., Campbell, J.: Extraction of drainage networks by using the consistent labeling technique. Remote Sensing of Environment 18, 163–175 (1985)
8. Ichoku, C., Karnieli, A., Meisels, A., Chorowicz, J.: Detection of drainage channel networks on digital satellite images. Int. J. of Remote Sensing 17, 1659–1678 (1996)
9. Dillabaugh, C., Niemann, O., Richardson, D.: Semi-automated extraction of rivers from digital imagery. GeoInformatica 6, 263–284 (2002)
10. Soille, P.: Morphological Image Analysis: Principles and Applications, 2nd edn. Springer, Heidelberg (2003)
11. Lantuéjoul, C., Maisonneuve, F.: Geodesic methods in image analysis. Pattern Recognition 17, 177–187 (1984)
12. Soille, P.: Generalized geodesy via geodesic time. Pattern Recognition Letters 15, 1235–1240 (1994) Download a PDF preprint: `http://ams.jrc.it/soille/soille94.pdf`
13. Verbeek, P., Verwer, B.: Shading from shape, the eikonal equation solved by grey-weighted distance transform. Pattern Recognition Letters 11, 681–690 (1990)
14. Soille, P., Vogt, J., Colombo, R.: Carving and adpative drainage enforcement of grid digital elevation models. Water Resources Research 39, 1366 (2003)
15. Soille, P., Gratin, C.: An efficient algorithm for drainage networks extraction on DEMs. J. of Visual Communication and Image Representation 5, 181–189 (1994)
16. Soille, P.: On morphological operators based on rank filters. Pattern Recognition 35, 527–535 (2002)

17. Soille, P.: Advances in the analysis of topographic features on discrete images. In: Braquelaire, A., Lachaud, J.-O., Vialard, A. (eds.) DGCI 2002. LNCS, vol. 2301, pp. 175–186. Springer, Heidelberg (2002)
18. Colombo, R., Vogt, J., Soille, P., Paracchini, M., de Jager, A.: On the derivation of river networks and catchments at European scale from medium resolution digital elevation data. Catena (2007), Available online (November 22, 2006)
19. Grazzini, J., Chrysoulakis, N.: Extraction of surface properties from a high accuracy DEM using multiscale remote sensing techniques. In: Proc. of the 19th Conf. Informatics for Environmental Protection, Brno, Czech Republic, pp. 352–356 (2005)